LUND UNIVERSITY

Membrane emulsification modelling: how can we get from characterisation to design?

Rayner, Marilyn; Trägårdh, Gun

Published in:
Desalination

DOI:
10.1016/S0011-9164(02)00403-4

2002

Link to publication

Citation for published version (APA):
Rayner, M., & Trägårdh, G. (2002). Membrane emulsification modelling: how can we get from characterisation to design? *Desalination*, *145*, 165-172. https://doi.org/10.1016/S0011-9164(02)00403-4

Total number of authors:
2

General rights
Unless other specific re-use rights are stated the following general rights apply:
Copyright and moral rights for the publications made accessible in the public portal are retained by the authors and/or other copyright owners and it is a condition of accessing publications that users recognise and abide by the legal requirements associated with these rights.
• Users may download and print one copy of any publication from the public portal for the purpose of private study or research.
• You may not further distribute the material or use it for any profit-making activity or commercial gain
• You may freely distribute the URL identifying the publication in the public portal

Read more about Creative commons licenses: https://creativecommons.org/licenses/

Take down policy
If you believe that this document breaches copyright please contact us providing details, and we will remove access to the work immediately and investigate your claim.

LUND UNIVERSITY

PO Box 117
221 00 Lund
+46 46-222 00 00

Download date: 04. Jul. 2025

ELSEVIER

Desalination 145 (2002) 165–172

DESALINATION

www.elsevier.com/locate/desal

Membrane emulsification modelling: how can we get from characterisation to design?

Marilyn Rayner*, Gun Trägårdh

Food Engineering, Lund University, PO Box 124, 221 00 Lund, Sweden
Tel. +46 (46) 2229820 Fax +46 (46) 2224622; email: marilyn.rayner@livstek.lth.se

Received 1 February 2002; accepted 15 February 2002

Abstract

There has been an increasing interest in a new technique for making emulsions known as membrane emulsification, which uses a microporous membrane operated in cross-flow. The continuous phase is pumped along the membrane and sweeps away dispersed phase droplets forming from pore openings as shown in Fig. 1. The effects of process parameters in membrane emulsification have been studied, especially on a quantitative level. However, the physical mechanisms of droplet formation are still under investigation to better elucidate the roles of operating parameters, and finally model the process. This work reviews current developments and deficiencies in the modelling membrane emulsification processes.

Keywords: Membrane emulsification; Modelling; Forces; Interfacial viscoelasticity; Operating parameters

1. Introduction

Emulsification is an important unit operation used in the pharmaceutical, food, and cosmetic industries. Membrane emulsification is a relatively new membrane technology which allows the production of emulsion droplets under controlled conditions with a narrow droplet size distribution. Both oil-in-water and water-in-oil emulsions are possible depending on the type of membrane used, as is the ability to form double emulsions; however, this work will focus on oil-in-water emulsions. The key feature of the membrane emulsification process which sets it apart from conventional emulsification technologies is that the size distribution of the resulting droplets is primarily governed by the choice of membrane and not by the development of turbulent drop break-up [1]. The main advantages of membrane emulsification are the possibility to produce droplets of a defined size with a narrow size distribution, low shear stress,

*Corresponding author.

Presented at the International Congress on Membranes and Membrane Processes (ICOM), Toulouse, France, July 7–12, 2002.

0011-9164/02/$– See front matter © 2002 Elsevier Science B.V. All rights reserved
PII: S0011-9164(02)00403-4

the potential for lower energy consumption, and simplicity of design [2].

Characterisation is essential in understanding new processes. Observing outcomes of a process using different operating parameters and ingredients yields valuable insight into underlying mechanisms. The language of mathematics is then applied to describe the relationship between the inputs and outputs of the process in a model. This model can subsequently be put to use as a tool to either predict in advance the outcome of a process or better still, design a process to produce a specific outcome, thus reducing the amount of trial-and-error work. This obvious progression is how most new processes are taken from being a laboratory curiosity to an industrial application. Membrane emulsification is not expected to be an exception (Fig. 1).

Droplet formation in membrane emulsification can be described through the characterisation of the detachment and retaining mechanisms, which arise from operating parameters (transmembrane pressure, cross-flow velocity), physical properties of the membrane (pore size, hydrophobicity, geometry) and properties of the ingredients to be emulsified (viscosity, interfacial tension, density). Not all parameters have equal relevance over the range of operating conditions and many have coupled effects. Modelling work that has been specifically aimed at membrane emulsification has included force balances, torque balances, and recently simulations using CFD. This work is important in understanding the relationships between outcomes and parameters; however, more knowledge concerning membrane design, interfacial phenomena, and hydrodynamics is required for general process design.

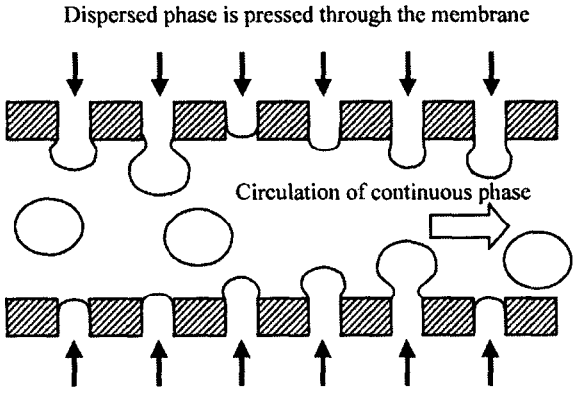

Fig. 1. Principle of membrane emulsification.

2. Summary of prior art

Most of the earliest work began with the modelling of bubbles and immiscible drops formed at submerged orifices in a quiescent continuous phase at dispersed phase velocities below jetting. These models embody various degrees of complexity such as the inclusion of different stages in droplet growth, flow during detachment process, and the effects of surfactants. Prediction and measurement of size and frequency of dispersion drops have been described by Scheele and Meister [3], Kumar and Kuloor [4], Karagannis et al. [5], and Tudose and Cârstea [6]. Skelland and Slaymaker [7] studied the effects of surface-active agents on the drop size predictions using Scheele and Meister's model. These models have been validated against data where droplets are forming at orifices in the millimetre range without liquid cross-flow, which makes the direct application of these models to membrane emulsification difficult. There are several works on bubbles forming in a cross-flow system [8–10], but bubble formation differs from liquid–liquid systems in that buoyancy effects are much more pronounced and the dispersed phase is easily compressible.

Modelling droplet formation specifically in a membrane emulsification process has been undertaken, and in each case the important process parameters with respect to droplet size were studied. Peng and Williams [1] used a high-speed video camera to observe droplet formation from single capillary pores ranging in size from 5 to 200 μm mounted in a wide rectangular

chamber. Schröder and Schubert [11–13] used microporous aluminum oxide membranes tubes 7 mm ID, having an effective length of 227 mm and average pores sizes 0.1 to 3 μm. They determined the droplet size distribution of the resulting emulsions with a Malvern Mastersizer. Abrahamse et al. [14] performed a numerical simulation using computational fluid dynamics of the dispersed phase flow out of 5 μm pore into a laminar cross-flow field.

3. Theory and governing phenomena

Drop sizes depend on several parameters including the physical properties of the system, dimensions, and flow rates. The droplet size of the resulting emulsion has been related to the pore size by a linear relationship for a given set of operating conditions:

$$D_d = \chi \cdot D_p \tag{1}$$

where χ can range typically from 2 to 10 [15,16].

The flux of the dispersed phase through the membrane is determined by the volume flow rate of oil through the pores and is assumed to follow Darcy's Law [17]. This flow depends on the difference between the applied pressure to the dispersed phase and the pressure drops or resistances to flow. In order for the oil to begin to permeate, the membrane the applied pressure must be higher than the sum of the average pressure in the continuous phase, P_{cts}, and the capillary pressure, P_{cap}, which are defined as follows:

$$P_{cap} = \frac{4\gamma \cos\theta}{D_p} \tag{2}$$

$$\bar{P}_{cts} = \frac{P_{cts1} - P_{cts2}}{2} \tag{3}$$

where P_{cts1} and P_{cts2} are the pressures in the continuous phase at both ends of the membrane module. The trans-membrane pressure, ΔP_{tm}, is often given as the difference between either side of the membrane. In a one-phase system, this trans-membrane pressure would arise from hydraulic losses alone; however, in the case of membrane emulsification, there is the added effect of the curved interface of oil at the pore mouth giving rise to P_{cap}. Thus in some cases the effective trans-membrane pressure, ΔP_{eff} [18] is given when describing the dispersed phase flux :

$$\Delta P_{tm} = P_{dis} - \bar{P}_{cts} \tag{4}$$

$$\Delta P_{eff} = \Delta P_{tm} - P_{cap} \tag{5}$$

$$J_{dis} = \frac{Q_{dis}}{A_{mem}} = \frac{\beta \Delta P_{eff}}{\mu_{dis} \cdot X_{mem}} \tag{6}$$

where β is a factor that depends on the membrane structure, i.e., pore size, shape, and frequency.

The effects of process parameters on drop size have been evaluated by associating them to forces acting on the system [1,13]. The main forces (shown in Fig. 2) that have been identified in the literature are described below. The interfacial tension force, F_γ, represents the effects

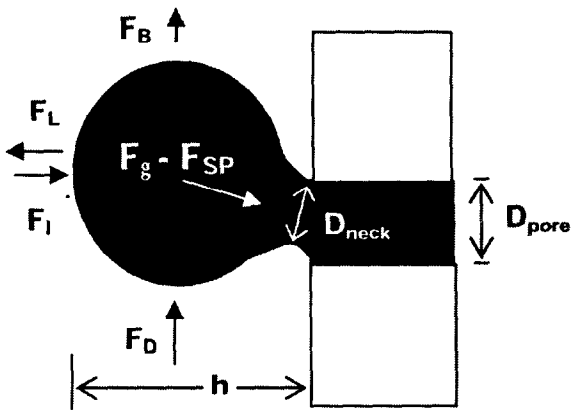

Fig. 2. Forces acting on a droplet forming at a pore.

effects of dispersed phase adhesion around the edge of the pore opening and is the key retaining force during droplet formation. The static pressure difference force, F_{SP}, is due to the pressure difference between the dispersed phase and the continuous phase at the membrane surface. The viscous drag force, F_D, is created by the continuous phase flowing past the droplet parallel to the membrane surface. The dynamic lift force, F_L, results from the asymmetric velocity profile of the continuous phase near the droplet. The buoyancy force, F_B, is due to the density difference between the phases. The inertial force, F_I, is associated with a mass of the fluid flowing out from the opening of the pore.

The relative magnitude of these forces changes as the droplet increases in size and has been plotted in the literature [1,13]. It has been shown that for micron-scale droplets the inertia and buoyancy forces are approximately 9 and 6 orders of magnitude smaller, respectively, than the drag and interfacial tension forces and therefore can be neglected in the force balance type models. In the case of larger droplets on the 200 μm scale, buoyancy effects become more important and have been included in the torque balance model of Peng and Williams [1]. They propose a torque balance between the drag, buoyancy, and the interfacial tension force assuming that the droplet is considerably deformed towards the membrane, as observed in their images where k_x =1.7 and corrects for a sphere in contact with a solid wall [1].

$$F_D + F_B = F_\gamma \tag{7}$$

$$F_D = k_x 6\pi \cdot R_d^2 \cdot \tau_w \tag{8}$$

$$F_B = \frac{4}{3}\pi \cdot R_d^3 \cdot \Delta\rho \cdot g \tag{9}$$

$$F_\gamma = 2\pi\gamma \cdot R_p \tag{10}$$

Schröder and co-workers [13,17] state that over the range of operating conditions in their set-up, only the interfacial tension force, the dynamic effect of the pressure difference between the phases, and the drag of the continuous phase have to be taken into account. They define these forces as follows:

$$F_\gamma = \pi \cdot D_{neck} \cdot \gamma_{(t)} \tag{11}$$

$$F_D = \frac{3}{2}\pi \cdot D_d^2 \cdot \tau_w \tag{12}$$

$$F_{SP} = \left(p_{dis} - p_{cts}\right) \cdot A_{neck} = \frac{4 \cdot \gamma_{(t)}}{D_d} \cdot \frac{\pi D_{neck}^2}{4} = F_\gamma \frac{D_{neck}}{D_d} \tag{13}$$

As seen above, they consider the dynamic interfacial tension of different emulsifiers measured by the bursting membrane method [19] on the 10^{-2} to 10^{1} second range. This covers the range of droplet formation times cited in the literature [1,12]. Wang et al. [17] use the above model as a starting point and include the effects of differing the continuous phase viscosity in their calculations for wall shear stress and diffusion of emulsifiers.

How well these models fit the data is hard to determine or compare. Peng and Williams [1] give an example of droplets forming from a 45 μm capillary under low wall shear stress (the cross-flow velocity is limited by imaging constraints) and their plotted model fits with significant agreement up to 0.4 m/s. In scaled-up experiments [20] they compare frequency distributions between pores and resulting drops. Although Schröder et al. [13] and Wang et al. [17] use the more elaborate model, they do not fit their experimental data against it. Using a ratio of F_γ to F_D plotted against wall shear stress is one way to estimate the relative size of their effects

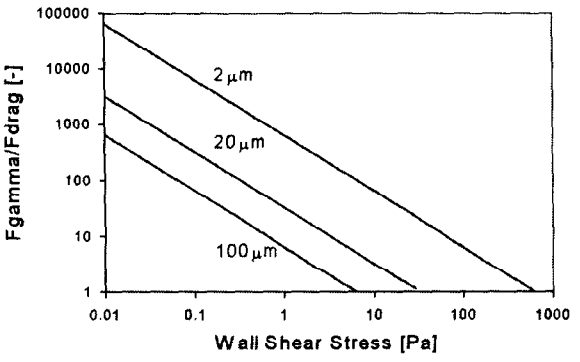

Fig. 3. Force ratio diagram. By moving horizontally in this plot the scale can be increased in both size (D_p) and time (reducing the continuous phase flow velocity generating the wall shear stress) while maintaining an equivalent force ratio on each scale.

over a wide range of drop sizes (Fig. 3). Taking the ratio of these forces equal to unity, the predicted drop size is plotted with experimental values taken from Joscelyne and Trägårdh [18] (Fig. 4). The model does follow the overall trend in the data; however, it diverges dramatically with different experimental conditions. With this as a background, what is possible to improve the description of the process, and the comparability of results?

4. Analysis of areas for improvement

4.1. Geometrical considerations in experimental set-ups

The wall shear stress generates the drag force on the droplet and is one of the key process parameters, thus must be well described and controlled in experimental work. In many cases the results are presented as a function of cross-flow velocity. This makes the resulting drag effect of the flow dependent on the diameter of the tube or channel. Another geometrical consideration that should be taken into account are entry effects. If there is an abrupt change in geometry in a flow loop, a certain distance in the new section is required before the flow is

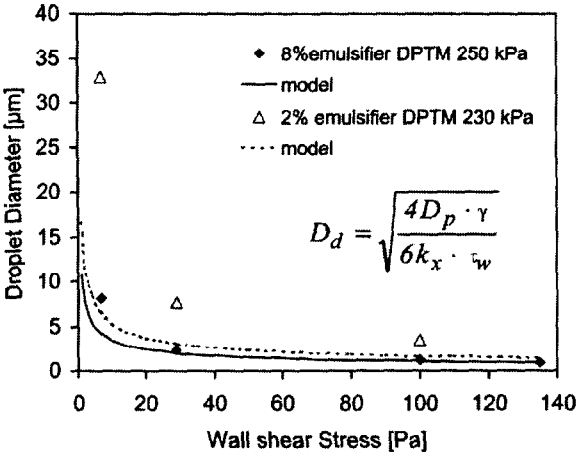

Fig. 4. Predicted and experimental drop sizes.

redeveloped. This causes pressure losses and local differences in the velocity and shear profile. For example, the entry length can reach 194 mm before flow is redeveloped when a sudden contraction in geometry occurring in a 7 mm ID tube with a cross-flow velocity of 1.2 m/s. For a piping system this would be negligible, but when using a 250-mm-long membrane tube it can have a significant effect. This of course can be easily remedied by inserting a straight pipe section of equal ID of the membrane tube with an appropriate length for the flow velocity used.

4.2. Membrane properties

At present, cross-flow membrane emulsification has been studied using tubular membranes made out of micro-porous glass (MPG), Shirasu porous glass (SPG), ceramic α-Al_2O_3, and ceramic α-Al_2O_3 coated with titania oxide or zirconia oxide. These membranes have been developed with separation processes in mind and thus are not necessarily optimal for membrane emulsification, even though promising results have been obtained with them. One often mentioned drawback of simply using separation membranes in this application is their high porosity. It has been postulated that there is coalescence of growing drops at the membrane

surface due to active pores being too close to one another and thus increasing the heterogeneity of drop sizes. However, due to the capillary pressure changing as a function of droplet radius, active pores may inhibit the flow out of neighbouring pores, thus greatly decreasing the effective porosity. To add to this, there is some size distribution among the pores making it likely that the largest pores are the most active, and the distribution of active pores will change as a function of applied pressure. The degree of these effects is yet to be fully explained. One approach to overcome this complexity is with numerical CFD studies using idealised geometry such as presented by Abrahamse et al. [14]. They calculate a maximum theoretical porosity taking into account both the drop pore ratio and the deformation of the growing drop. These studies could be verified against experimental work using model membranes having a custom-made pore size and pattern. Two possible candidates are laser-drilled, stainless-steel sheets [21] or inorganic microfiltration membranes made using laser interference lithography and silicon micro-machining technology [22].

4.3. How to describe the interfacial phenomena

Interfacial tension is another aspect of membrane emulsification which needs careful consideration. Membrane emulsification differs from conventional processes in that the droplet formation time is of the same order of magnitude as the dynamic interfacial tension of common food emulsifiers [19]. The effect of emulsifiers is further complicated by the fact that droplet deformation and adsorption at the interface are coupled, thus giving the surface viscoelastic properties. Thus both the rate at which deformation and detachment forces act, as well as how fast surfactants adsorb to the growing interfacial area becomes relevant over the time scales involved. This coupling effect limits the application of the force balance model since it will not give a definite break-off criteria. The effect of surface viscoelasticity on drop formation could be described by a time constant relating the velocity gradient in the continuous phase near the drop to the relaxation time of the interface.

4.4. Pressures

The pressure applied to the dispersed phase must overcome P_{cap} and P_{cts}, leaving the remaining pressure, ΔP_{eff} to drive the flow through the pores. P_{cts} is defined as an average due to the pressure drop along the membrane tube. A droplet forming near the inlet will experience a higher continuous phase pressure and as a consequence, a smaller ΔP_{eff} than a droplet forming near the outlet. The relative size of this pressure drop compared to the effective transmembrane pressure, given as a percentage, is calculated for a number of experimental conditions and shown in Table 1.

$$\varepsilon_r\,\% = \frac{4\tau_w \cdot L_{mem}}{\Delta P_{eff} \cdot D_{mem}} \tag{14}$$

This relative difference is large in some cases, but may not have an equally large effect on the

Table 1
Relative difference in pressure, ε_r% for a variety of wall shear stresses and ΔP_{tm}

ΔP_{tm}, kPa	Pore diam., μm	ε_r, % Wall shear stress [Pa]			
		5	29	100	135
100	0.5	0.9	5.1	17.4	24
	0.2	1.3	7.7	27	36
	0.1	8.9	52	180	240
250	0.5	0.3	1.8	6.2	8.3
	0.2	0.4	2.0	7.0	9.5
	0.1	0.5	2.6	9.0	12

Emulsifier 8% Dimodan PVP, D_{mem} = 7 mm; L_{mem} = 250 mm [18].

droplet size distribution. These effects increase with increasing length of membrane tubes, and should be considered during scale-up. This potential local deviation in the pressure driving the dispersed phase flux can be minimised by choosing appropriate operating parameters.

5. Conclusions

In order to develop a predictive model for membrane emulsification processes, more work is required. Droplet detachment is more complicated than originally thought, but can be studied further by taking surface viscoelastic properties into account. The most important parameters in process design are well known and insight into their coupled effects will improve modelling work. With improved modelling and design, a number of interesting industrial applications can be realised such as controlled release system in parentheral pharmaceuticals and micro-encapsulation of flavours. Due to the low shear stresses and mild processing conditions, shear sensitive materials could be incorporated into a variety of novel formulations.

6. Symbols

A_{neck}, A_{mem} — Area: droplet neck, membrane, m^2

D_d, D_p

D_{mem}, D_{neck} — Diameter: drop, pore, membrane tube, droplet neck, m

J_{dis} — Dispersed phase flux, m/s

L_{mem} — Length: membrane tube, m

P_{cap}, P_{cts}, P_{dis}, ΔP_{eff}, ΔP_{tm} — Pressure: capillary, continuous phase, dispersed phase, effective, trans-membrane, Pa

Q_{dis} — Volume flow, m^3/s

R_d, R_p — Radius: drop, pore, m

X_{mem} — Membrane thickness, m

Greek

ε_r — Relative difference of pressures

γ — Interfacial tension, N/m

μ — Viscosity, Pa.s

θ — Contact angle, °

$\Delta\rho$ — Density difference between phases, kg/m^3

τ_w — Wall shear stress, Pa

References

[1] S.J. Peng and R.A. Williams, Chem.Eng.Res.Des., 76 (1998) 894–901.

[2] H. Schubert, Proc. ICEF 7, Brighton UK, Academic Press, 1997, pp. AA82–AA87.

[3] G.F. Scheele and B.J. Meister, AIChE J., 14(1) (1968) 9–15.

[4] R. Kumar and N.R. Kuloor, in: T.B. Drew, G.R. Cokelet, J.W. Hoopes and T. Vermeulen, eds., Advances in Chemical Engineering, Vol. 8, Academic Press, 1970.

[5] C. Karagiannis, D. Papageorgiou and M. Stamatoudis, Can. J. Chem. Eng., 72 (1994) 13–15.

[6] R.Z. Tudose and S. Cârstea, Hungarian J. Ind. Chem., 22 (1994) 15–21.

[7] A.H.P. Skelland E.A. Slaymaker, Ind. Eng. Chem. Res., 29 (1990) 494–499.

[8] Y. Kawase and J.J. Ulbrecht, Ind. Eng. Chem. Process Des. Dev., 20 (1994) 636–640.

[9] H.K. Nahra and Y. Kamotani, Chem. Eng. Sci., 55 (2000) 4653–4665.

[10] R.B.H. Tan, W.B. Chen and K.H. Tan, Chem. Eng. Sci., 55 (2000) 6259–6267.

[11] V. Schröder and H. Schubert, in: Food Emulsions and Foams, Royal Society of Chemistry, Cambridge, 1999, pp. 70–80.

[12] V. Schröder and H. Schubert, Colloids and Surfaces, 152 (1999) 103–109.

[13] V. Schröder, O. Behrend and H. Schubert, J. Colloid Int. Sci., 202 (1998) 334–340.

[14] A.J. Abrahamse, A. van der Pradt, R.M. Boom and W.B.C. Heij, AIChE J., 47(6) (2001) 1285–1291.

[15] R. Katoh, Y. Asano, A. Furuya, K. Sotoyama and M. Tomita, J. Membr. Sci., 113 (1996) 131–135.

[16] Y. Mine, M. Shimizu and T. Nakashima, Colloids and Surfaces B, 6 (1996) 261–268.

[17] Z. Wang, S. Wang, V. Schröder and H. Schubert, Chinese J. Chem. Eng., 8 (2000) 108–112.
[18] S.M. Joscelyne and G. Trägårdh, J. Food Eng., 39 (1998) 59–64.
[19] M. Stang, H. Kardstein, and H. Schubert, Chem. Eng. Process, 33 (1994) 307–311.
[20] S.J. Peng, and R.A. Williams, Chem. Eng. Res. Design, 76 (1998) 902–938.
[21] P.J. Dowding, J.W. Goodwin and B. Vincent, Colloids and Surfaces A, 180 (2000) 301–309.
[22] S. Kuiper, C.J.M. van Rijn, W. Nijdan and M.C. Elwenspoek, J. Membr. Sci., 150 (1998) 1–8.